Spontaneous Symmetry Breaking in the Formation of a Dinuclear Gadolinium Semiquinonato Complex: Synthesis, High-Field EPR Studies, and Magnetic Properties

Andrea Dei,[a] Dante Gatteschi,*[a] Carlo A. Massa,[b] Luca A. Pardi,[b] Sandrine Poussereau,[a] and Lorenzo Sorace[a]

Abstract: The synthesis and characterisation of an asymmetric dinuclear gadolinium(III) semiquinonato complex, namely $[Gd_2(HBPz_3)_2(dtbsq)_4]\cdot CHCl_3$ (**1**; $HBPz_3$ = hydrotris(pyrazolyl)borate, dtbsq = 3,5-di-*tert*-butyl-*o*-semiquinone), is reported. The crystal structure of **1** was determined at room temperature. It crystallises in the triclinic system $P\bar{1}$, with $a = 16.735(5)$ Å, $b = 17.705(5)$ Å, $c = 19.553(5)$ Å, $\alpha = 99.680(5)^\circ$, $\beta = 109.960(5)^\circ$, $\gamma = 107.350(5)^\circ$, $Z = 2$ and $R = 9.96$. The structure of **1** consists of a dinuclear asymmetric unit in which the two gadolinium(III) ions have coordination numbers of eight and nine. Three of the dioxolene molecules act as asymmetric bridging ligands, while the fourth molecule behaves as a bidentate ligand towards a single metal ion. The magnetic properties of **1** were investigated by means of susceptibility measurements and high-field electron paramagnetic resonance (HF-EPR) spectroscopy. They revealed an $S = 0$ ground spin state with excited states of higher spin very close in energy and a small negative zero-field splitting with a transverse anisotropy term for a $S = 7$ state.

Keywords: EPR spectroscopy · gadolinium · lanthanides · magnetic properties · N ligands · semiquinones

Introduction

Molecules that are characterized by high-spin electronic ground states are being actively investigated as possible candidates in the development of molecular-based materials of technological interest.[1–13] Within this framework, the chemistry of metal-semiquinonato adducts is particularly attractive, since both the metal acceptor and the donor ligand can be paramagnetic. The nature of the magnetic coupling in 3d metal complexes formed by semiquinonato ligands is reasonably clear as far as the 1:1 adducts are concerned.[14, 15] In particular, these paramagnetic ligands have been observed to have stronger couplings than other organic radicals, such as nitroxides, on account of their higher coordination ability. Further semiquinonato complexes have also been observed to give relatively large zero-field splitting of the ground S states, presumably as a result of large anisotropic exchange interactions.[16] This feature is important if single molecule magnets are desired. Up to now, there have been considerably fewer investigations of rare-earth ions. In principle they might yield interesting compounds because they can provide both very high spin [$S = 7/2$ for gadolinium(III)] and large anisotropy.

We have recently reported the synthesis, structure and magnetic studies of the mononuclear compound $[Gd(HBPz_3)_2(dtbsq)]\cdot 2\,CHCl_3$ ($HBPz_3$ = hydrotris(pyrazolyl)borate, dtbsqQ = 3,5-di-*tert*-butyl-*o*-semiquinone).[17] This complex has the strongest antiferromagnetic coupling to gadolinium(III) so far known. We have explained this phenomenon by suggesting a non-negligible overlap between the magnetic orbitals of the radical and the *f* orbitals of the rare-earth ion, on account of the strong donor nature of the semiquinonate ligand. In order to extend our investigations to the design and synthesis of gadolinium semiquinonato systems that contain more than two interacting magnetic centres, we have attempted to obtain a mononuclear bis(semiquinonato)gadolinium complex. Following this approach, solid compounds of formula $[Gd(HBPz_3)(dtbsq)_2]$ were obtained as different solvates.

The chloroform solvate provided crystals of acceptable quality for an X-ray diffraction structure analysis and showed that the correct formula is $[Gd_2(HBPz_3)_2(dtbsq)_4]$ (**1**). The dinuclear unit is asymmetric, therefore an unusual symmetry breaking occurs in solution. This may open new possibilities for the synthesis of high-spin molecules. We wish to report here the structure and the magnetic properties of **1**.

[a] Prof. D. Gatteschi, Prof. A. Dei, Dr. S. Poussereau, Dr. L. Sorace
Dipartimento di Chimica università di Firenze
Via Maragliano 75/77, 50144 Firenze (Italy)
Fax: (+39) 55-354845
E-mail: gattesch@chim1.unifi.it

[b] Dr. C. A. Massa, Dr. L. A. Pardi
Istituto di Fisica Atomica e Molecolare—C.N.R.
Via Alfieri 1, 56100 Ghezzano (Italy)

  0947-6539/00/0624-4580 $ 17.50+.50/0

Results and Discussion

Synthesis: Blue microcrystalline powders of $[Gd(HBPz_3)(dtbsq)_2]$ stoichiometry precipitate when mixtures of a gadolinium(III) salt, potassium hydrotris(pyrazolyl)borate and 3,5-di-*tert*-butyl-*o*-catechol are allowed to react in a 1:1:2 ratio in basic methanol. Charge balance considerations suggest the presence of two semiquinone ligands. This is confirmed by the electronic spectrum in dichloromethane which shows a large band at 13000 cm^{-1} ($\varepsilon = 1045\ M^{-1}cm^{-1}$), and a pattern of bands at higher energy, the most intense centred at 26700 cm^{-1} ($\varepsilon = 6965\ M^{-1}cm^{-1}$), another one at 27900 cm^{-1} ($\varepsilon = 6340\ M^{-1}cm^{-1}$) and a shoulder at 29000 cm^{-1}. All these bands have been assigned as internal transitions in the semiquinonato ligand.[17, 18]

Recrystallisation at low temperature in a hexane/chloroform mixture allows the formation of blue crystals of formula $[Gd_2(HBPz_3)_2(dtbsq)_4]\cdot CHCl_3$ (**1**). The formula was determined by X-ray crystal structure analysis as described below. Similar solvates were obtained from dichloromethane and 1,2-dichloroethane. In all the solvents investigated, we always observed the formation of the dinuclear complex; this suggests that **1** is thermodynamically favoured with respect to the mononuclear complex with the same gadolinium: semiquinone ratio. Unfortunately, the reactivity of this complex, as well as its solubility, strongly limited our investigations in other solvents.

Molecular structure: No really good crystals could be isolated from the solutions, notwithstanding numerous attempts. Therefore, the X-ray crystal structure determination is of low quality. It cannot be used to describe fine details; however, it certainly provides a sufficient frame for the description of the magnetic properties.

The ORTEP view of the crystal structure of **1** is shown in Figure 1. Crystallographic data and selected interatomic distances and angles for **1** are presented in Tables 1 and 2, respectively. As mentioned above, the molecular unit is dinuclear. The complex is asymmetric and the two metal ions exhibit two different coordination numbers. The coordination number of Gd1 is eight, with a geometry which can be described as a distorted square antiprism, while Gd2 is surrounded by nine donor atoms which define a distorted tricapped trigonal prism. The asymmetry is also associated with the semiquinone ligands: three of them are bridging, with one of their oxygen atoms bound to both gadolinium(III) ions in a μ-1,2 fashion, while the other oxygen is bound to only one metal ion. The fourth semiquinone ligand is bound to only one metal ion (Figure 2). This asymmetric type of ligation has already been reported for both catecholate and semiquinone complexes formed by these ligands with transition metal ions.[15] The coordination polyhedron around Gd1 is defined by three nitrogen atoms and four oxygen atoms of two chelating semiquinones, and one oxygen atom of the third semiquinone. The coordination polyhedron of Gd2 is defined by three nitrogens of hydrotris(pyrazolyl)borate, two oxygens of the non-bridged semiquinone, two μ-1,2-bridging oxygens of two different semiquinones and the other two oxygens of the third bridging semiquinone.

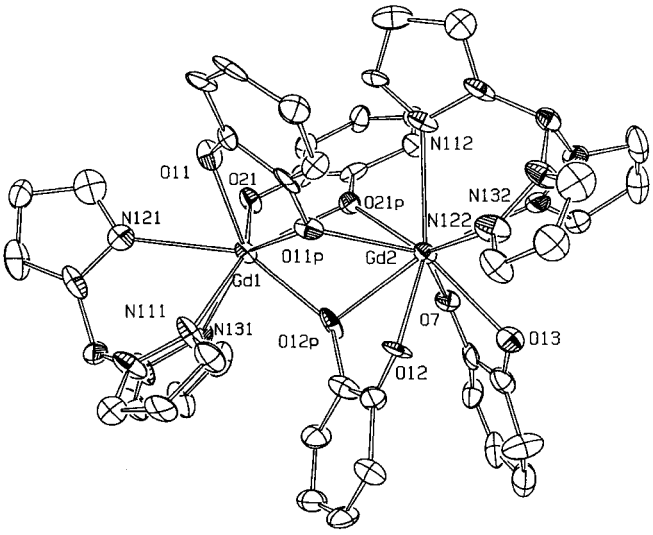

Figure 1. ORTEP view of **1**. Thermal ellipsoids are shown at 25% probability for clarity. For the same reason, hydrogen atoms and *tert*-butyl groups were omitted.

Table 1. Crystal data and structure refinement for **1**.

formula	$C_{75}H_{104}B_2Cl_3Gd_2N_{12}O_8$
M_w	1740.55
T [K]	293(2)
λ[Å]	0.71069
crystal system	triclinic
space group	$P\bar{1}$, $P1$
a [Å]	16.735(5)
b [Å]	17.705(5)
c [Å]	19.553(5)
α [°]	99.680(5)
β [°]	109.960(5)
γ [°]	107.350(5)
V [Å^3]	4956.8(24)
Z	2
ρ_{calcd} [Mg m^{-3}]	1.165
μ [mm^{-1}]	1.455
θ range [°]	2.50–22.04
index ranges	$-17 \le h \le 16$ $-18 \le k \le 18$ $0 \le l \le 20$
reflections collected	12661
independent reflections	12179 [R(int) = 0.0760]
reflections observed [$I > 2\sigma$(I)]	6222
data/restraints/parameters	12167/0/863
goodness-of-fit on F^2	1.012
final R indices [$I > 2\sigma(I)$]	$R1 = 0.0997$, $wR2 = 0.2683$
R indices (all data)	$R1 = 0.2193$, $wR2 = 0.3262$

The Gd1–Gd2 bond length (3.755 Å) is shorter than that usually observed in gadolinium dimers reported in the literature;[19, 20] however, it is somewhat longer than the Gd–Gd bond length recently reported in a dinuclear complex synthesised with phenolate ligands.[21]

Usually, the oxidation state of dioxolene units bound to metal ions is derived from the values of the distances between the two oxygen-bound carbons and from C–O links.[15] Interestingly, the bond lengths found here for the chelating nonbridging semiquinonate are in agreement with those reported for the analogous 1:1 Gd:semiquinonate mononuclear complex.[17] The C–C bond lengths in that complex are

Table 2. Bond lengths [Å] and angles [°] in **1**.

Gd1−O12P	2.28(2)	O12P-Gd1-O21	112.5(5)	O7-Gd2-O13	66.4(5)
Gd1−O21	2.349(14)	O12P-Gd1-O11	134.7(5)	O7-Gd2-O12	102.5(5)
Gd1−O11	2.37(2)	O21-Gd1-O11	91.8(5)	O13-Gd2-O12	63.2(5)
Gd1−O21P	2.395(14)	O12P-Gd1-O21P	68.3(5)	O7-Gd2-O21P	74.1(5)
Gd1−O11P	2.450(14)	O21-Gd1-O21P	66.1(5)	O13-Gd2-O21P	140.3(5)
Gd1−N111	2.48(2)	O11-Gd1-O21P	89.9(5)	O12-Gd2-O21P	125.0(5)
Gd1−N121	2.56(2)	O12P-Gd1-O11P	68.9(5)	O7-Gd2-O11P	127.0(5)
Gd1−N131	2.59(2)	O21-Gd1-O11P	129.0(5)	O13-Gd2-O11P	137.8(5)
Gd2−O7	2.375(15)	O11-Gd1-O11P	66.1(5)	O12-Gd2-O11P	74.6(5)
Gd2−O13	2.42(2)	O21P-Gd1-O11P	68.4(5)	O21P-Gd2-O11P	66.8(5)
Gd2−O12	2.416(13)	O12P-Gd1-N111	80.1(6)	O7-Gd2-O12P	66.6(5)
Gd2−O21P	2.457(15)	O21-Gd1-N111	150.5(6)	O13-Gd2-O12P	96.1(5)
Gd2−O11P	2.492(13)	O11-Gd1-N111	97.3(6)	O12-Gd2-O12P	64.9(4)
Gd2−O12P	2.517(14)	O21P-Gd1-N111	141.4(6)	O21P-Gd2-O12P	63.8(5)
Gd2−N132	2.53(2)	O11P-Gd1-N111	80.1(6)	O11P-Gd2-O12P	64.7(5)
Gd2−N122	2.58(2)	O12P-Gd1-N121	146.8(6)	O7-Gd2-N132	77.4(6)
Gd2−N112	2.66(2)	O21-Gd1-N121	81.4(6)	O13-Gd2-N132	73.0(5)
O11P−C611	1.30(3)	O11-Gd1-N121	71.2(6)	O12-Gd2-N132	131.1(5)
O11−C111	1.24(3)	O21P-Gd1-N121	141.9(6)	O21P-Gd2-N132	102.3(5)
C111−C611	1.54(3)	O11P-Gd1-N121	126.7(5)	O11P-Gd2-N132	143.9(5)
O21−C121	1.29(2)	N111-Gd1-N121	75.3(7)	O12P-Gd2-N132	143.6(6)
O21P−C621	1.30(2)	O12P-Gd1-N131	84.2(6)	O7-Gd2-N122	137.8(6)
C121−C621	1.40(3)	O21-Gd1-N131	79.4(6)	O13-Gd2-N122	76.2(6)
O12P−C612	1.39(3)	O11-Gd1-N131	139.5(5)	O12-Gd2-N122	75.9(5)
O12−C112	1.25(3)	O21P-Gd1-N131	120.8(5)	O21P-Gd2-N122	141.6(6)
C112−C612	1.41(3)	O11P-Gd1-N131	146.2(6)	O11P-Gd2-N122	93.8(6)
O13−C2Q	1.26(3)	N111-Gd1-N131	75.4(7)	O12P-Gd2-N122	138.8(5)
O7−C1Q	1.27(3)	N121-Gd1-N131	68.5(6)	N132-Gd2-N122	73.5(6)
C1Q−C2Q	1.48(3)	Gd1-O11P-Gd2	98.9(4)	O7-Gd2-N112	123.6(5)
		Gd1-O21P-Gd2	101.4(6)	O13-Gd2-N112	136.6(6)
		Gd1-O12P-Gd2	102.9(6)	O12-Gd2-N112	133.7(5)
				O21P-Gd2-N112	70.2(5)
				O11P-Gd2-N112	74.3(5)
				O12P-Gd2-N112	127.1(6)
				N132-Gd2-N112	69.6(6)
				N122-Gd2-N112	72.8(6)

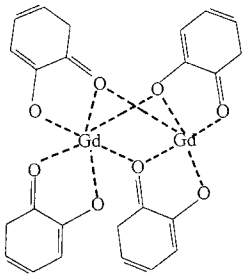

Figure 2. Bonding scheme of semiquinones and gadolinium ions in **1**.

slightly larger and the C−O ones slightly shorter than those usually observed in semiquinonate complexes of transition metal ions.[15] For the bridging semiquinones, the C−O bond lengths that involve the μ-1,2 bridging oxygens are long (1.30(3), 1.30 (2), 1.39 (3) Å), while the bonds that involve the nonbridging oxygens are shorter (1.24(3), 1.29(2), 1.25(3) Å). The corresponding C−C bonds vary from 1.40(3) to 1.54(3) Å. It is apparent that, given the poor quality of the structure determination and the complex nature of the molecule, the bond lengths alone cannot provide unambiguous evidence of the nature of the dioxolene ligands. Additional evidence is obtained from the analysis of the HF-EPR and magnetic data to be described below. Considering this, and the complexity of the structure of **1**, with dioxolene units bridging between gadolinium ions, attention must be paid when the oxidation state of the bridging ligands is derived from the values of these bond lengths. However, the investigations carried out on complex **1** in the solid state which are discussed below remove any ambiguity about the presence of only radical ligands.

As far as we know, this is the first structure reported of a dinuclear unit that involves both a rare-earth ion and a paramagnetic ligand. A similar asymmetric structure which contains gadolinium(III) ions has been recently described; however, this involved a diamagnetic hexadentate ligand.[21] According to the classical chemical view, this complex can be regarded as a donor–acceptor self-adduct of an amphiphilic molecule. However, it should be stressed that, in general, these interactions lead to a symmetric di- or polynuclear adduct and not to an asymmetric structure, as observed in this case.[15] We believe that the asymmetric nature of this complex may therefore allow the synthesis of heterodinuclear derivatives as a result of a simple acid–base reaction. The structure of the resulting products should be dictated by the difference in the acidities of the two different metal acceptors.

High-field electron paramagnetic resonance (HF-EPR) spectroscopy: Because of the complexity of the X-band EPR spectrum recorded at 4.2 K, which turned out to be impossible to interpret, we chose to use HF-EPR to obtain information on the anisotropy and ground spin state of **1**. HF-EPR spectroscopy has already proved to be one of the most powerful techniques to gain this kind of information.[22–24] One of the main advantages in the use of this technique is that the high fields strongly simplify the spectra, since zero-field splitting (ZFS) can be treated, in first approximation, as a perturbation of the Zeeman effect. Additionally, the high fields allow direct measurement of the sign of the ZFS and, if all the transitions are observed, they allow, at low temperature, the exact determination of the nature of the ground spin state.

Figure 3 shows the HF-EPR spectra of **1** recorded at 240 GHz and different temperatures ranging from 200 K to 4.2 K. At 200 K, there is essentially one broad band centred at $g = 2$ as expected for a system that contains gadolinium(III) and semiquinones. Two satellites are located symmetrically around the central band. As the temperature is decreased, the spectrum shows more features: at 10 K a fine-structure

0947-6539/00/0624-4582 $ 17.50+.50/0 *Chem. Eur. J.* **2000**, *6*, No. 24

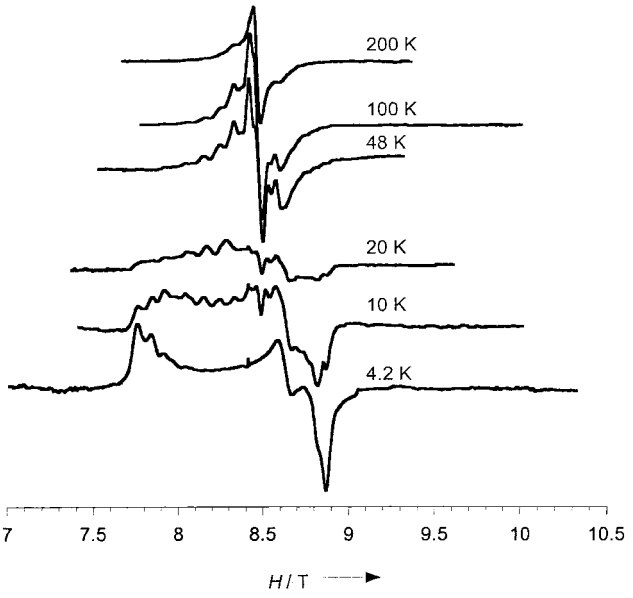

Figure 3. Temperature evolution of HF-EPR spectra of **1** recorded at 240 GHz between 200 K and 4 K.

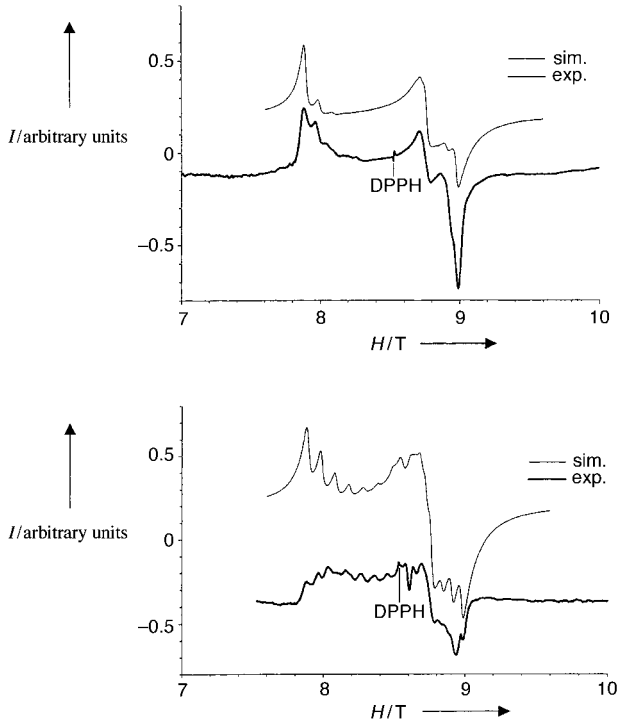

Figure 4. Comparison of simulated and experimental (bold) HF-EPR spectra of **1** at 4 K (top) and 10 K (bottom). The corresponding spin hamiltonian parameters are given in the text.

progression is clearly resolved at low field. The spectrum at 4.2 K shows the typical simplification expected for a high-field EPR experiment.[23, 24] In fact, since the Zeeman energy is larger than kT at low temperature, only the lowest M_S states will be populated and one transition, $-S \rightarrow -S+1$, is observed. The spectrum at 4.2 K shows a feature at $\approx$7.87 T and two additional features at $\approx$8.8 and 9.0 T, which can be attributed to the $1-S \rightarrow -S+1$ transitions with the external field parallel to z, x and y respectively. The additional features at $\approx$7.95 T and 8.03 T correspond to the z component of the $-S+1 \rightarrow -S+2$ and $-S+2 \rightarrow -S+3$ transitions, respectively. The fact that the z transitions are observed at low field indicates that this is the easy axis, thus suggesting a negative axial anisotropy zero-field splitting parameter D.[23, 24] A regular fine structure is clearly observed in the parallel region of the spectrum recorded at 10 K, with a 0.088 T separation between two successive peaks. This behaviour indicates a high-spin state, with the higher energy M_S states that are depopulated on as the temperature decreases. An S ground state should show, in the strong field limit, $2S$ transitions separated in the parallel region by $2D$, with S above and below the centre of the spectrum. If we consider that the low-field parallel region is extended for 0.66 T, and that the separation between neighbouring lines is $\approx$0.088 T, a ground spin state $S=7$, and a D value of -0.044 T (-0.047 cm^{-1}) are clearly indicated.

We then tried to simulate the spectra at 4.2 K and 10 K starting from these parameters. The simulations were performed by means of a program, written by Weihe,[25] which calculates the energy levels from exact diagonalisation of the spin hamiltonian matrix for each value of the magnetic field and each orientation, and then calculates the spectrum from the transition probability. The best simulations (Figures 4) were obtained with $S=7$, $g_{iso}=2.00$, $D=-0.0465$ cm^{-1}, $E=0.0052$ cm^{-1}, in good agreement with the parameter values which were estimated in the preliminary analysis of the spectra. However, the introduction of a small transverse anisotropy term ($E/D \cong 0.11$), which mainly affects the perpendicular region of the spectra, proved to be necessary in order to obtain correct simulations. The temperature evolution of the spectra, as well as the position of the lines, is well reproduced, even if the appearance of excited state transitions at 10 K makes the simulation process incomplete. The presence of transitions from excited states at this rather low temperature is the reason why it is not possible to reproduce the spectra at higher temperatures. The conclusion that the HF-EPR allows us to reach is that there is an $S=7$ state, which is either the ground state or is very close to it.

Magnetic measurements: The plot of χT versus T between 2.5 K and 300 K is shown in Figure 5. The high-temperature value of 17.24 emu K mol^{-1} is in agreement with two $S=\frac{5}{2}$ and four $S=\frac{1}{2}$ independent spin carriers with $g=2.00$ (theoretical value 17.25 emu K mol^{-1}), as expected from the crystal structure. This is a confirmation of the assignment of the dioxolene molecules as semiquinones. Other assignments, such as two semiquinones, one cathecholate and one quinone would require $\chi T=16.5$ emu K mol^{-1}. Since the overall coupling is antiferromagnetic, as evidenced by the temperature dependence of χT to be described below, a high-temperature limit higher than the limit for noninteracting spins would be impossible to justify. The decrease of the χT product on decreasing temperature indicates the existence of antiferromagnetic interactions between the different paramagnetic centres. However, the quite high value at low temperature (10.97 emu K mol^{-1} at 2.5 K) and the slow decrease of χT seem to indicate an incomplete spin compensation.

  0947-6539/00/0624-4583 $ 17.50+.50/0

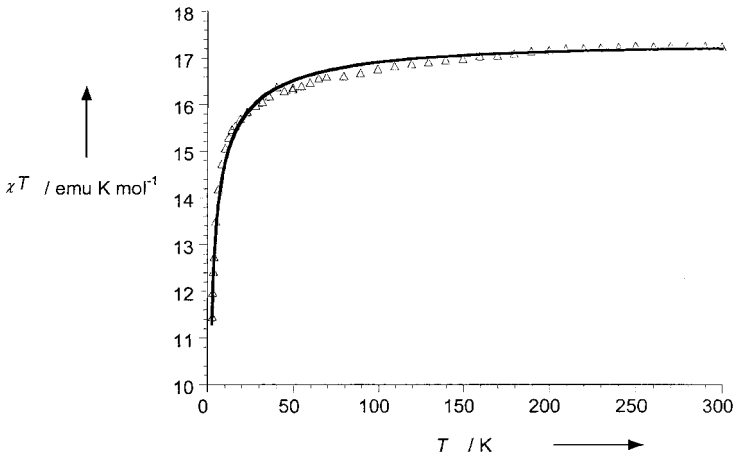

Figure 5. χT vs. T curve measured between 2.5 K and 300 K for **1** and best-fit curve. Best-fit parameters are reported in the text.

The M versus H curves measured for **1** at two temperatures are shown in Figure 6. The high-field value of 13.7 μ_B observed at 2.4 K is slightly lower than that expected for an $S=7$ ground state (14 μ_B). This seems to indicate that $S=7$ is the ground state in a field of 6 T. However, the initial

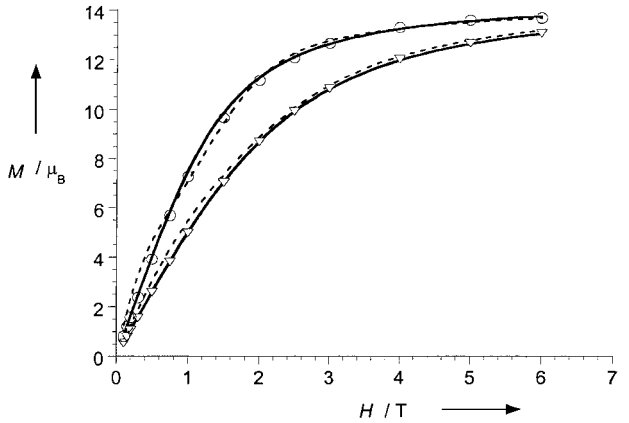

Figure 6. Magnetisation curves for **1** measured at 2.4 K (○) and 4.7 K (▽). The dashed lines are the best simulations obtained assuming an $S=7$ ground state, while the continuous lines were obtained assuming an $S=0$ ground state.

magnetisation at low field is much smaller than that expected for $S=7$, which suggests that other spin states of lower S values are populated at low field. The combined picture emerging from the analysis of the HF-EPR spectra, of the magnetic susceptibility and of magnetisation is that in zero field there is an $S=7$ multiplet, which is either the ground state or is close to the ground state. In any case, there must be several multiplets with $S<7$ that are thermally populated at 4 K.

In order to try to fit the temperature dependence of χT, simplifying assumptions are needed. A possible coupling is shown in Figure 7.

In order to reduce the number of parameters employed in the simulation, the three bridging semiquinonate (SQ) ligands were taken as magnetically equivalent in the interaction with gadolinium ions and with the same scope, all the semi-

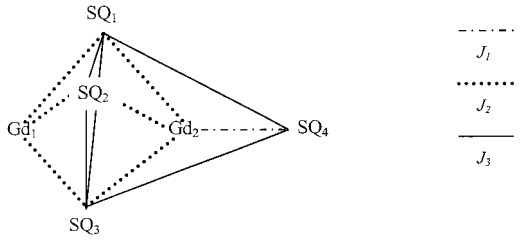

Figure 7. Coupling scheme for **1**. For the second fit an additional interaction involving the two gadolinium ions was considered.

quinonate–semiquinonate interactions were taken as equivalent to each other. Additionally, we neglected the Gd–Gd interaction; this is justified on the basis of literature data, which show only a very small value for this coupling.[19, 20] The following isotropic exchange hamiltonian[26] [Eq. (1)] was then used to simulate the χT vs T curve.

$$H=J_1(\boldsymbol{S}_{Gd2}\cdot\boldsymbol{S}_{SQ4})+J_2(\boldsymbol{S}_{Gd2}\cdot\boldsymbol{S}_{SQ1}+\boldsymbol{S}_{Gd2}\cdot\boldsymbol{S}_{SQ2}+\boldsymbol{S}_{Gd2}\cdot\boldsymbol{S}_{SQ3}+\boldsymbol{S}_{Gd1}\cdot\boldsymbol{S}_{SQ1}+\boldsymbol{S}_{Gd1}\cdot\boldsymbol{S}_{SQ2}+\boldsymbol{S}_{Gd1}\cdot\boldsymbol{S}_{SQ3})+J_3(\boldsymbol{S}_{SQ1}\cdot\boldsymbol{S}_{SQ2}+\boldsymbol{S}_{SQ1}\cdot\boldsymbol{S}_{SQ3}+\boldsymbol{S}_{SQ1}\cdot\boldsymbol{S}_{SQ4}+\boldsymbol{S}_{SQ2}\cdot\boldsymbol{S}_{SQ4}+\boldsymbol{S}_{SQ3}\cdot\boldsymbol{S}_{SQ4}+\boldsymbol{S}_{SQ2}\cdot\boldsymbol{S}_{SQ3}) \quad (1)$$

A Weiss correction[27] was introduced to provide a better reproduction of the low-temperature values; the same behaviour may be explained with the introduction of a small ZFS term, as found for the HF-EPR spectra. The introduction of a θ value is then purely phenomenological and does not necessarily imply interactions between neighbouring dinuclear units (the shortest intermolecular Gd–Gd and Gd–O distances are 12.6 Å).

The best-fit curve (continuous line, Figure 6) was obtained with the following parameters: $J_1=2.51$ cm^{-1}, $J_2=-0.6$ cm^{-1}, $J_3=18.15$ cm^{-1} and $\theta=-0.12$ K. A second fit was attempted introducing the Gd–Gd interaction; this adds a $J_{Gd1,Gd2}\boldsymbol{S}_{Gd1}\cdot\boldsymbol{S}_{Gd2}$ term to the hamiltonian given in Equation (1) and neglecting θ. In fact a non-zero Gd–Gd interaction was needed in order to justify the highly frustrated nature of the ground state in a previously reported Gd-NITR radical one-dimensional compound (NITR = 2-R-4,4,5,5-tetramethyl-4,5-dihydro-1*H*-imidozolyl-1-oxyl 3-oxide; R = ethyl, isopropyl).[28] The best-fit curve obtained is perfectly superimposed over the first one, and the value for the coupling constants are in qualitative agreement with the first fit: $J_1=1.75$ cm^{-1}, $J_2=0.35$ cm^{-1}, $J_3=12.85$ cm^{-1}, $J_{Gd1,Gd2}=0.08$ cm^{-1}.

With the values of the coupling constants derived from the first fit, the ground state is a doubly degenerate $S=7$ state with excited states ranging from $S=6$ to $S=0$ (all of them doubly degenerate) which are within 1.3 cm^{-1}. The $S=8$ state (12.2 cm^{-1} above the ground state) and the $S=9$ (55 cm^{-1} above the ground state) are higher in energy. On the other hand, the values of the coupling constants of the second fit require an $S=0$ ground state (because of the antiferromagnetic coupling between the two gadolinium ions) and the excited states ranging from $S=1$ to $S=7$ are within 2.7 cm^{-1} in energy. Again in this case the $S=8$ (17.4 cm^{-1}) and the $S=9$ (48.5 cm^{-1}) states are higher in energy. Both of these results are in qualitative agreement with the interpretations of the HF-EPR spectra and with the magnetisation data.

0947-6539/00/0624-4584 $ 17.50+.50/0 *Chem. Eur. J.* **2000**, *6*, No. 24

We tried to discriminate between these two results and attempted a simulation of the magnetisation curves, taking into account the population of the seven lower energy states—as derived from the two different fits of the susceptibility data—and ZFS effects for ground and excited states. The first simulation was performed by considering the relative energies of the spin states as derived from the first fit. In the application of the ZFS parameters derived from HF-EPR to the $S=7$ ground state, we were forced to use quite large ZFS ($D=-0.3\ cm^{-1}$) for lower S spin states in order to obtain some agreement with the experimental curves. However, even with the use of these values, the quality of the simulation was not very good (Figure 6, dashed lines).

If one considers the energy levels derived from the second fit of the susceptibility data, a value of ZFS for lower S spin states which is comparable ($0.04\ cm^{-1}$) with that derived from HF-EPR for $S=7$ is obtained for the best-fit curve. It should be noted that in this case the quality of the simulation is good (Figure 6, continuous line). This is then a very strong indication in favour of a spin ground state $S=0$, with $S=7$ very close in energy. In principle it would be possible to include a higher number of J parameters to allow for the low symmetry of the compound. However, we do not feel that a reliable determination of their values can be achieved.

The values of the coupling constants obtained from the susceptibility fit deserve some comments. The coupling constant between Gd2 and the chelating semiquinonate is smaller than that recently reported for a similar mononuclear complex ($J=11.15\ cm^{-1}$)[17] with 1:1 Gd/semiquinonate stoichiometry. The difference in the coupling may be attributed to different factors: i) the difference in coordination sphere around Gd, which is eight-coordinate in the mononuclear complex; ii) the existence of interactions involving both Gd2 and the chelating semiquinonate with the other paramagnetic centres of the complex. This may reduce the strength of the J_1 interaction.

The very low value of J_2 may be explained by considering that i) each of three semiquinonates are bound to the two Gd ions and ii) the average bridged semiquinonate–Gd bond lengths are larger than those of the chelating radical. This strongly reduces the overlap between the *f* orbitals of the rare-earth ions with the magnetic orbital of the radicals, which is known to be a key factor in determining the nature and the magnitude of magnetic interactions.[17, 21, 30] Finally, the quite high value of the semiquinonate–semiquinonate coupling constant indicates that gadolinium ions are effective in transmitting the antiferromagnetic interaction as it has already been noted with nitronyl-nitroxide radicals.[13, 28]

Conclusions

We have obtained the first dinuclear complex between Gd^{III} ions and paramagnetic ligands. Its structure has been resolved by X-ray diffraction studies and shows an asymmetric unit: Gd1 and Gd2 have coordination number of eight and nine, respectively. Moreover, there are two coordination modes between the dioxolene ligands and Gd ions: three radicals bridge the rare-earth ions through a single oxygen atom, the fourth is only bound to the Gd2 ion. These two ways of linking seem to be intimately correlated to the magnitude of the magnetic interaction between gadolinium ions and the radicals; the coupling is weaker for bridging semiquinonate ligands interacting with Gd ions than between the chelating radical and the Gd2 ion.

The magnetic anisotropy of an excited state of **1** was determined by HF-EPR spectroscopy, while magnetisation measurements were crucial for the assignment of the ground spin state as $S=0$. It may be concluded that such a geometrical arrangement of gadolinium and paramagnetic ligands is not favourable to obtain an antiferromagnetic coupling larger than those previously reported. To gain better insight into the results of this investigation, efforts to isolate the mononuclear analogue of **1** are currently in progress.

Experimental Section

$[Gd_2(HBPz_3)_2(dtbsq)_4]\cdot CHCl_3$: A solution of 3,5-di-*tert*-butyl-*o*-catechol (0.444 g, 2 mmol) in methanol (10 mL) was added to a white suspension of $GdCl_3\cdot 6H_2O$ (0.371 g, 1 mmol) and hydrotris(pyrazolyl)borate (0.252 g, 1 mmol) in methanol (20 mL) under argon. After 20 minutes of stirring, solid KOH was added (2 mmol, 0.112 g) to this solution. As soon as the KOH had dissolved, the solution was filtered in air to allow the oxidation of the catechol into semiquinone and the elimination of KCl. A blue powder appeared which was filtered and washed with cold methanol. Suitable crystals for X-ray analysis were obtained after recrystallisation in an hexane/$CHCl_3$ solution (10:1; 20 mL) at low temperature ($-30\,^{\circ}C$). Elemental analysis calcd (%) for $Gd_2C_{75}H_{101}B_2O_8N_{12}Cl_3$: C 51.71, H 5.85, N 9.65; found: C 51.97, H 5.66, N 9.53.

Crystallography: A small crystal of **1** ($0.15\times 0.15\times 0.3$ mm) was sealed in a glass capillary containing a small amount of solvent. Data collection was made on a four-circle CAD4 ENRAF NONIUS diffractometer, $Mo_{K\alpha}$ radiation ($\lambda=0.71069$ Å) graphite monochromator, $\omega-2\theta$ scan, 293 K. Intensities were corrected for absorption (ψ scan). The system was found to crystallise in a triclinic lattice. Structure was successfully solved by direct methods by using SIR92[31] both for $P1$ and $P\bar{1}$. Because of the large number of parameters involved, refinement was performed only in the $P\bar{1}$ space group. Remaining atoms were identified by means of successive Fourier difference syntheses with SHELXL 93.[32] The structure was refined against F^2 with full-matrix least-squares refinement with 12179 independent reflections (of which 6222 observed, $[I>2\sigma(I)]$), no restraints and 863 parameters. Anisotropic thermal factors were used for 86 of 102 non-hydrogen atoms. 98 hydrogen atoms were placed in calculated positions. The relatively high value of the residual electronic density, located near gadolinium ions, may be attributed to satellite peaks. As the final R value was quite high, we tried to refine the structure by carrying out the absorption correction through DIFABS, after location of all non-hydrogen isotropic atoms. The structure refined in such a way showed only a minor improvement (R $(I>2\sigma)=9.58\,\%$, maximum density peak $=2.46\ e\ Å^{-3}$) with respect to that obtained through ψ-scan correction and no significant differences in angles and distances.

Crystallographic data (excluding structure factors) for the structure reported in this paper has been deposited with the Cambridge Crystallographic Data Centre as supplementary publication No. CCDC-144025. Copies of the data can be obtained free of charge on application to CCDC, 12 Union Road, Cambridge CB21EZ, UK (fax: (+44) 1223-336-033; e-mail: deposit@ccdc.cam.ac.uk)

Magnetic measurements: Magnetic susceptibility of a polycrystalline powder of **1** was measured between 2 and 300 K in an applied magnetic field of 0.1 and 1 T by means of a Cryogenic S600 SQUID magnetometer. Data were corrected for the magnetism of the sample holder, which was determined separately in the same temperature range and field, and diamagnetism correction was estimated from Pascal's constants. Magnetisation measurements were performed on the same sample at 2.5 and 4.5 K with field up to 6 T.

HF-EPR spectra: HF-EPR spectra were recorded at the High-Field High-Frequency Electromagnetic Resonance Laboratory hosted by IFAM-CNR in Pisa. The instrument has a superconducting magnet (Oxford Instruments), a home-built CO_2-pumped millimeter laser (MML) and a fast indium antimonide hot-electron bolometer (QMC Instruments) cooled to liquid helium temperature as a detector. The measurements were performed with a field sweep rate of 0.2 T min^{-1} at 239.1 GHz (with CH_3I as the laser gas) on ground microcrystalline powder pressed to a pellet together with *n*-eicosane to avoid orientation of the sample. Field calibration was obtained with the 1,1-diphenyl-2-picrylhydrazyl (DPPH) radical as the reference.

Acknowledgements

This work was supported by the 3MD EU Network (Contract No.: ERB 4061 PL 97-0197).

[1] A. Dei, D.Gatteschi, *Inorg. Chim. Acta* **1992**, *198–200*, 813.
[2] C. J. O'Connor, *Research Frontiers in Magnetochemistry* (Ed: C. J. O'Connor), World Scientific, Singapore, **1993**.
[3] O. Kahn, *Molecular Magnetism*, VCH, New York, **1993**.
[4] *Magnetic Molecular Materials* (Eds: D. Gatteschi, O. Kahn, J. S. Miller, F. Palacio), Kluwer Academic, Dordrecht, **1991**.
[5] O. Kahn, Y. Pei, Y. Journaux in *Inorganic Materials* (Eds: D. W. Bruce, D. O'Hare), Wiley, New York, **1996**.
[6] R. Sessoli, H. L. Tsai, A. R. Schake, S. Y. Wang, J. B. Vincent, K. Folting, D. Gatteschi, G. Christou, D. N. Hendrickson, *J. Am. Chem. Soc.* **1993**, *115*, 1804.
[7] D. P. Goldberg, A. Caneschi, S. J. Lippard, *J. Am. Chem. Soc.* **1993**, *115*, 9299.
[8] J. S. Miller, A. J. Epstein, *Angew. Chem.* **1994**, *106*, 399; *Angew. Chem. Int. Ed. Engl.* **1994**, *33*, 385.
[9] H. O. Stumpf, L. Ouahab, Y. Pei, P. Bergerat, O. Kahn, *J. Am. Chem. Soc.* **1994**, *116*, 3866.
[10] J. K. McCusker, C. A. Christmas, P. M. Hagen, R. K. Chadha, D. F. Harvey, D. N. Hendrickson, *J. Am. Chem. Soc.* **1991**, *113*, 6114.
[11] E. Libby, J. K. McCusker, E. A. Schmitt, K. Folting, D. N. Hendrickson, G. Christou, *Inorg. Chem.* **1991**, *30*, 3486.
[12] C. A. Christmas, H. L. Tsai, L. Pardi, J. M. Kesselman, P. K. Gantzel, R. K. Chadha, D. Gatteschi, D. F. Harvey, D. N. Hendrickson, *J. Am. Chem. Soc.* **1993**, *115*, 12483.
[13] C. Lescop, D. Luneau, E. Beloritzky, P. Fries, M. Guillot, P. Rey, *Inorg. Chem.* **1999**, *38,* 5472.
[14] J. K. McCusker, H. G. Jang, S. Wang, G. Christou, D. N. Hendrickson, *Inorg. Chem.* **1992**, *31*, 1874.
[15] a) C. G. Pierpont, C. W. Lange, *Prog. Inorg. Chem.* **1994**, *41*, 331; b) C. G. Pierpont, R. M. Buchanan, *Coord. Chem. Rev.* **1981**, *38*, 45.
[16] A. Dei, D. Gatteschi, L. Pardi, A. L. Barra, L. C. Brunel, *Chem. Phys. Lett*. **1990**, *175*, 589.
[17] A. Caneschi, A. Dei, D. Gatteschi, L. Sorace, K. Vostrikova, *Angew. Chem.* **2000**, *112*, 252; *Angew. Chem. Int. Ed. Engl.* **2000**, *39*, 246.
[18] C. Benelli, A. Dei, D. Gatteschi, L. Pardi, *Inorg. Chem.* **1989**, *28*, 3089.
[19] S. Liu, L. Gelmini, S. J. Rettig, R. C. Thompson, C. Orvig, *J. Am. Chem. Soc.* **1992**, *114*, 6081.
[20] A. Panagiotopoulos, T. F. Zafiropoulos, S. P. Perlepes, E. Bakalbassis, I. Masson-Ramade, O. Kahn, A. Terzis, C. P. Raptopoulou, *Inorg. Chem.* **1995**, *34*, 4918.
[21] I. A. Setyawati, S. Liu, S. J. Rettig, C. Orvig, *Inorg. Chem.* **2000**, *39*, 496.
[22] A. L. Barra, D. Gatteschi, R. Sessoli, *Chem. Eur. J.* **2000**, *6*, 1608.
[23] A. L. Barra, L.-C. Brunel, D. Gatteschi, L. Pardi, R. Sessoli, *Acc. Chem. Res.* **1998**, *31*, (8), 460.
[24] A. L. Barra, A. Caneschi, D. Gatteschi, R. Sessoli, *J. Am. Chem. Soc.* **1995**, *117*, 8855.
[25] C. J. H. Jacobsen, E. Pedersen, J. Villadsen, H. Weihe, *Inorg. Chem.* **1993**, 1216.
[26] J. H. Van Vleck, *The Theory of Magnetic and Electric Susceptibilities*, Oxford University Press, London, **1932**.
[27] C. J. O'Connor, *Prog. Inorg. Chem.* **1982**, *29*, 203.
[28] a) C. Benelli, A. Caneschi, D. Gatteschi, L. Pardi, P. Rey, *Inorg. Chem.* **1990**, *29*, 4223; b) C. Benelli, D. Gatteschi, R. Sessoli, A. Rettori, M. G. Pini, F. Bartolomé, J. Bartolomé, *J. Magn. Magn. Mat.* **1995**, *140–144,* 1649.
[29] M. Andruh, I. Ramade, E. Codjovi, O. Guillou, O. Kahn, J. C. Trombe, *J. Am. Chem. Soc.* **1993**, *115*, 1822.
[30] C. Benelli, A. Caneschi, O. Guillou, L. Pardi, D. Gatteschi, *Inorg. Chem.* **1990**, *29*, 1750.
[31] A. Altomare, G. Cascarano, C. Giacovazzo, A. Guagliardi, M. C. Burla, G. Polidori, M. Camalli, *J. Appl. Chem.* **1994**, *27*, 435.
[32] G. M. Sheldrick, *SHELXL-93*, *Program for Crystal Structure Refinement*, University of Göttingen, Göttingen (Germany), **1993**.

Received: May 12, 2000 [F2483]

  0947-6539/00/0624-4586 $ 17.50+.50/0